

- Pan, Y. H., and A. H. Oort, 1983: Global climate variations connected with sea surface temperature anomalies in the eastern equatorial Pacific Ocean for the 1958–73 period. *Mon. Wea. Rev.*, **111**, 1244–1258, doi:10.1175/1520-0493(1983)111<1244:GCVCWS>2.0.CO;2.
- Power, S., T. Casey, C. Folland, A. Colman, and V. Mehta, 1999: Interdecadal modulation of the impact of ENSO on Australia. *Climate Dyn.*, **15**, 319–324, doi:10.1007/s003820050284.
- Reynolds, R. W., N. A. Rayner, T. M. Smith, D. C. Stokes, and W. Wang, 2002: An improved in situ and satellite SST analysis for climate. *J. Climate*, **15**, 1609–1625, doi:10.1175/1520-0442(2002)015<1609:AIISAS>2.0.CO;2.
- Risbey, J. S., S. Lewandowsky, C. Langlais, D. P. Monselesan, T. J. O’Kane, and N. Oreskes, 2014: Well-estimated global surface warming in climate projections selected for ENSO phase. *Nat. Climate Change*, **4**, 835–840, doi:10.1038/nclimate2310.
- Santer, B. D., and Coauthors, 2014: Volcanic contribution to decadal changes in tropospheric temperature. *Nat. Geosci.*, **7**, 185–189, doi:10.1038/ngeo2098.
- Schmidt, G. A., D. T. Shindell, and K. Tsigaridis, 2014: Reconciling warming trends. *Nat. Geosci.*, **7**, 158–160, doi:10.1038/ngeo2105.
- Stocker, T. F., and Coauthors, 2013: Technical Summary. *Climate Change 2013: The Physical Science Basis*. Stocker, T. F. et al. Eds., Cambridge University Press, 33–115.
- Tokinaga, H., and S.-P. Xie, 2011: Wave- and anemometer-based sea surface wind (WASWind) for climate change analysis. *J. Climate*, **24**, 267–285, doi:10.1175/2010JCLI3789.1.
- Trenberth, K. E., J. T. Fasullo, G. Branstator, and A. S. Phillips, 2014: Seasonal aspects of the recent pause in surface warming. *Nat. Climate Change*, **4**, 911–916, doi:10.1038/nclimate2341.
- Urabe, Y., and S. Maeda, 2014: The relationship between Japan’s recent temperature and decadal variability. *Sci. Online Lett. Atmos.*, **10**, 176–179, doi:10.2151/sola.2014-037.
- Watanabe, M., H. Shiogama, H. Tatebe, M. Hayashi, M. Ishii, and M. Kimoto, 2014: Contribution of natural decadal variability to global warming acceleration and hiatus. *Nat. Climate Change*, **4**, 893–897, doi:10.1038/nclimate2355.
- Xie P, and P. A. Arkin, 1997: Global precipitation: A 17-year monthly analysis based on gauge observations, satellite estimates and numerical model outputs. *Bull. Amer. Meteor. Soc.*, **78**, 2539–2558, doi:10.1175/1520-0477(1997)078<2539:GPAYMA>2.0.CO;2.
- Zhang, Y., J. M. Wallace, and D. S. Battisti, 1997: ENSO-like interdecadal variability: 1900–93. *J. Climate*, **10**, 1004–1020, doi:10.1175/1520-0442(1997)010<1004:ELIV>2.0.CO;2.

Warming the abyss: The deep ocean's contribution to global warming

Sarah Purkey¹, Damien Desbruyères², and Nathalie Zilberman³

¹Lamont-Doherty Earth Observatory, Columbia University

²National Oceanography Centre, United Kingdom

³Scripps Institution of Oceanography

The rate of increase of the global mean surface temperature has shown a high level of variability despite a steady increase in greenhouse gases, including periods of zero or relatively low warming, often referred to as a warming “hiatus” (e.g., Trenberth and Fasullo 2010; Foster and Rahmstorf 2011). During the hiatus periods the top of the atmosphere radiative imbalance has remained at roughly 1 W m^{-2} . This suggests that either the observational record of surface temperature is incorrect owing to under sampling or data corrections or the heat is accumulating in other parts of the climate system, raising the question of where this excess heat is going (Trenberth et al. 2009; Karl et al. 2015; Kosaka and Xie 2013).

In order to address this question and quantify the planetary heat gain, it is necessary to monitor all sinks of energy within the Earth’s climate system. Atmospheric warming only accounts for roughly 1% of the excess radiative heat gain, with the vast majority, approximately 93%, absorbed by the global oceans and the remaining 6% accounted for by warming land and melting ice (Rhien et al. 2013). Despite the large role the ocean plays in absorbing the excess heat, much of it remains unmonitored, and historical estimates of ocean heat content are mostly limited to the upper 700 m. Since the early 2000s, the Argo array has revolutionized ocean monitoring above 2000 m, however, the deep

(below 2000 m) and abyssal (below 4000 m) ocean remains sparsely sampled in space and time (Lyman and Johnson 2014).

The abyssal ocean communicates with the surface at high latitudes where deep and bottom waters are formed and fed into the bottom limb of the Meridional Overturning Circulation (MOC). North Atlantic Deep Water (NADW) is formed through open water convection in the Labrador and Nordic Seas when surface waters cool and sink (LeBel et al. 2008). In the Southern Ocean, Antarctic Bottom Water (AABW) is produced when cold, dense shelf water - formed through complex ice shelf-ocean interactions - flows down the Antarctic continental slope and mixes with ambient waters (Gordon 2009). While advective timescales for these waters to circulate from the surface through the bottom and deep limbs of the MOC is on the order of 1000s of years, dynamical effects can quickly communicate high latitude changes throughout the globe via isopycnal heave (e.g., Masuda et al. 2010). For example, a decrease in deep water formation rates at high latitudes will cause a deepening of isopycnals, appearing as a warming on isobars communicated via Rossby and Kelvin waves on decadal timescales (Kouketsu et al. 2009, 2011; Masuda et al. 2010; Purkey and Johnson 2012). Therefore, the deep ocean can increase its heat storage by either advection of warmer water or through a dynamical response.

Since the 1990s, the deep and abyssal oceans have been warming, contributing roughly 10% to the total ocean heat content (Purkey and Johnson 2010). However, limited deep ocean data only allows for estimates of decadal heat content trends, and makes it hard to assess short-term changes in the deep ocean's heat content, such as the change over the most recent hiatus period. Nonetheless, here we present a current assessment of deep and abyssal ocean heat content changes since the 1990s. We compare two studies: one covering 1990-2010 and the other 2000-2015 to show that there is little evidence that this rate has increased over the hiatus period. We end with a description of a proposed deep observing system that will allow for the necessary monitoring of the deep ocean in order to close ocean heat and sea level rise budgets over the next century.

Monitoring the abyss

High quality deep ocean temperature data are primarily limited to ship based hydrographic work. In the early 1990s, the international World Ocean Circulation Experiment (WOCE) Hydrographic Program completed a full-depth, high resolution oceanographic survey producing a climatological baseline for the deep ocean's hydrographic properties. The WOCE one-time survey occupied over 50 coast-to-coast zonal and meridional sections gridding the global ocean with high quality conductivity-temperature-depth

(CTD) profiles nominally every 55 km. An important subset of the WOCE sections have been reoccupied in support of the Climate Variability and Predictability (CLIVAR) and Carbon Cycle Science programs now coordinated by the international Global Ocean Ship Based Hydrographic Investigations Program (GO-SHIP), allowing for the first estimates of the variability in the global deep ocean heat content over recent decades.

Using all repeated sections between 1990 and 2010, Purkey and Johnson (2010) quantified the heat flux across the 2000 and 4000 m isobaths within 32 deep basins around the globe, which is required to account for the observed warming trend below 2000 and 4000 m, respectively (Figure 1a). Since the timing of the first and last occupation of the sections varies, the basin heat content for each basin is calculated over a slightly different time period, with a mean time period of 1993-2006. During this period a clear southern-intensified warming pattern emerged, with the Southern Ocean warming below 2000 m at a rate of 0.03 °C per decade, and a smaller, but statistically significant, warming to the north below 4000 m following the deep flow of AABW along the bottom limb of the MOC (Figures 1a; 2). The warming along isobars is equivalent

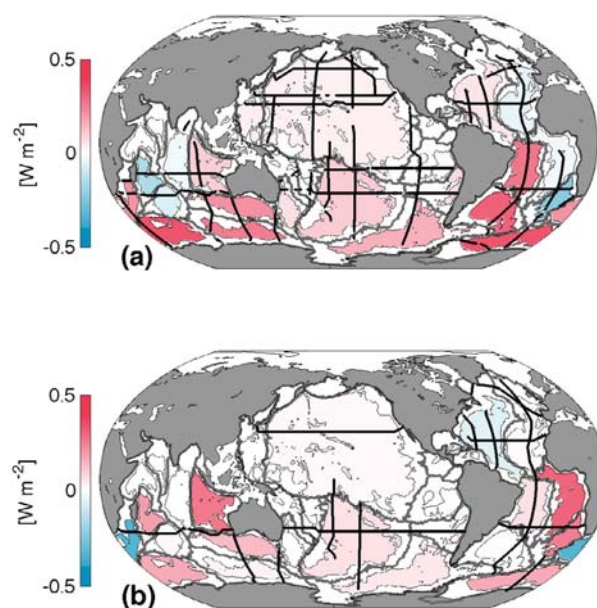


Figure 1: Basin (gray lines) mean local heat fluxes through 4000 m (color) implied by abyssal warming below 4000 m from the period centered around a) 1993-2006 and b) 2004-2013 with the location of repeated sections for each time period (black lines). Data for a) following Purkey and Johnson (2010) and b) following Desbruyères, McDonagh, and King (in prep.).

to a downward isotherm heave - or a volume loss of the cold, dense water - suggesting that the warming is being driven by a slowdown in the bottom limb of the MOC (Purkey and Johnson 2012). This total abyssal global ocean heat content change is equivalent to a heat flux of 0.03 W m^{-2} applied over the surface of the Earth. Including deep warming (2000-4000 m) increases the deep heat content to 0.07 W m^{-2} , mostly owing to warming in the deep Southern Ocean².

Following the Purkey and Johnson (2010) methodology, Desbruyères, McDonagh, and King (in prep.) derived a new estimate of deep ocean heat content post-2000, obtained from 18 hydrography sections occupied at least twice between 2001 and 2014. Comparing these two periods suggests weak variability in the magnitude and vertical structure of the trend between the 1990's and the mid-2010's. Between 2000-2014, the total deep heat flux remained at 0.07 W m^{-2} , with the deep layer accounting for a higher percentage of the total heat gain (Figure 2). Warming trends were primarily observed in the North Atlantic and Southern Ocean, and slightly damped by a cooling trend in the Pacific. After 2001, the warming signal was weaker within the bottom water (below 4000 m; Figure 2), and only accounted for a 0.025 W m^{-2} heat flux. Abyssal warming was, however, still observed in most ocean basins, making its contribution to the global heat flux of continued importance (Figure 1b).

Near source of deep water variability

The deep and abyssal changes around the globe can be traced back to their deep-water formation sites at high latitudes. NADW fills the deep and abyssal North Atlantic before flowing over the denser AABW in the South Atlantic and into the Antarctic Circumpolar Current (ACC). In the Pacific and Indian, the deep and abyssal ocean is primarily (over 50%) filled with AABW (Johnson 2008). These two water-masses dominate the global ocean below the thermocline, and

play a critical role in climate through deep ocean carbon and heat storage (Johnson 2008; Meehl et al. 2006).

NADW

The North Atlantic is seen as a key region for recent climate variability due to ventilation of the deep ocean with newly formed NADW. This basin is also among the most adequately sampled by hydrography sections (Figure 1). The deep and abyssal warming

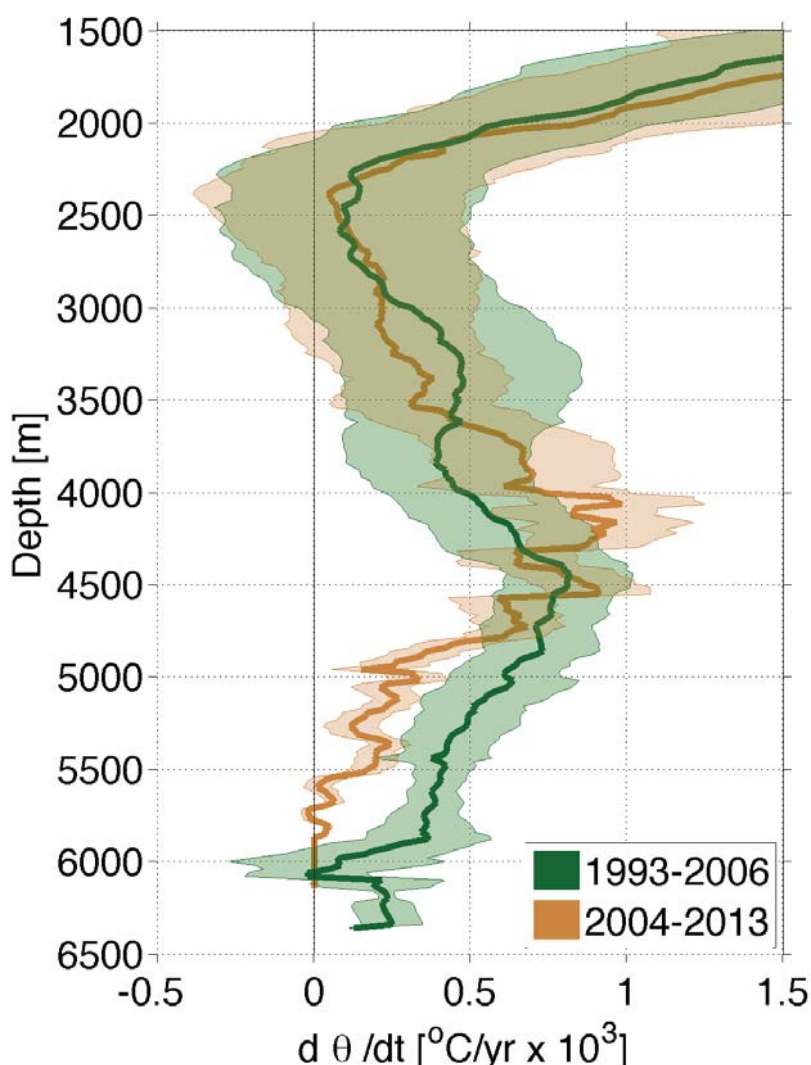


Figure 2: Global mean (thick lines) rate of change in potential temperature with 95% confidence intervals (shading) using repeated sections between 1990-2010 centered between 1993-2006 following Purkey and Johnson (2010; green) and repeated sections between 2001-2014 centered between 2004-2013 following Desbruyères, McDonagh, and King (in prep.; orange).

rate between 2000 and 2014 shows a predominant warming signal in the upper deep layer (0.03 ± 0.004 °C per decade between 2000 m and 3000 m) observed in both the western and eastern subpolar region (Desbruyères et al. 2014). This warming signal in the upper deep layer overlies an abyssal cooling signal of smaller magnitude (-0.004 ± 0.002 °C per decade; Figure 1b) primarily seen in the western subtropics – one of the main gateways for NADW to the Southern Hemisphere. Overall, the deep and abyssal North Atlantic warming rates during the period contribute to the global heat uptake by 0.017 ± 0.016 W m⁻².

Such opposing trends of the deep and abyssal regions may reveal the distinct forcing and timescales of the main NADW components: the Labrador Sea Water and the Greenland-Scotland Overflow Water. The former possesses a strong interannual and decadal response to atmospheric forcing and will be significantly influenced by wind-driven dynamics through its eastward and southward journey within the intermediate layers of the subpolar gyre (Desbruyères et al. 2014). Longer timescales will dominate at deeper levels, with changes in water-mass properties potentially becoming increasingly important.

AABW

The abyssal and deep Southern Ocean, filled with the most recently formed AABW, has warmed significantly between the 1990s and 2010s, albeit the warming rate has decreased in recent years (Figures 1 and 2). AABW warming in these southern basins has been attributed to multiple factors. In the South Pacific and South Indian, the Ross Sea Shelf Water, an important end member of AABW found in this region, has freshened at a rate of 0.03 PSU per decade since the 1950s, likely owing to the increase in glacial melt rates along West Antarctica (Jacobs and Giulivi 2010). The resulting freshening decreases the density and volume of the recently ventilated AABW, causing an apparent warming along isobars (Aoki et al 2005; Swift and Orsi 2012; Purkey and Johnson 2013; Katsumata et al. 2015). In the Weddell Sea, however, the bottom and deep waters have been warming and decreasing in volume with no freshening, possibly owing to changes in local wind stress spinning up and down the Weddell gyre (Fahrbach et al. 2004, 2011; Purkey and Johnson 2012, 2013; Jullion et al. 2010).

Conclusion

Multiple studies have suggested the recent warming hiatus is due to a vertical redistribution of heat toward the ocean bottom, and indeed there is evidence of a redistribution of heat from the

surface layer (upper 700 m) to intermediate depths (700-2000 m; e.g., Chen and Tung 2014). However, there is no pronounced change in the magnitude and vertical structure of temperature trends below 2000 m between the 1990-2010 and 2001-2014 periods, with both periods contributing 0.07 W m⁻² to the global heat budget (Figure 2). This warming accounts for about 10% of the total oceanic heat uptake estimate between 1993-2010 of 0.71 W m⁻² (Rhien et al. 2013). Together these estimates appear in line with a net downward radiative flux imbalance at the top of Earth's atmosphere of 0.62 ± 0.43 W m⁻², estimated from satellite data and atmospheric reanalyses between 2000 and 2012 (Allan et al. 2014).

Because of the importance of a deep ocean temperature record, a global ocean observing system is required to resolve temperatures from the top-to-bottom ocean and not just the upper-half of the water column. Upper-ocean sampling, largely carried out by the conventional Argo array, has nearly global coverage and resolves large-scale features on seasonal timescales. Since the end of 2007, Argo has reached its target of a sustained array of 3,300 floats at 3° x 3° spacing. The Argo array currently provides over 100,000 temperature and salinity profiles per year. Deep ocean hydrographic observations are limited to sparse shipboard hydrographic sections repeated roughly every decade, with a bias toward the summer time and high latitudes. Additionally, short-lived moored arrays of confined spatial coverage tend to be concentrated towards the coastline of continents in the Northern Hemisphere. Less than 100,000 profiles have been collected in the deep ocean since 1995.

The development of a new generation of deep-profiling Argo floats, capable of diving and recording temperature and salinity below 2000 m, is underway. The Deep Argo fleet consists of Deep Arvor and Deep NINJA floats designed to sample to 4000 m, and Deep APEX and Deep SOLO floats capable of reaching 6000 m (Figure 3). The primary focus of Deep Argo is to resolve interannual to decadal signals in deep ocean temperature, salinity, and circulation. The pilot implementation of regional Deep Argo arrays has begun in the Southern Ocean, the southwest Pacific Ocean, and the North Atlantic Ocean. The driving motivation for the Deep Argo deployments in the North Atlantic and Southern Oceans is to reduce uncertainties in deep water formation rates as well as to detect deep property changes. The rationale for implementing pilot arrays in the southwest Pacific Ocean is to quantify interannual variability in deep water mass characteristics and investigate pathways of water masses in the deep ocean. The pilot arrays are expected to continue for the next two to three years before transitioning to global implementation. Current plans include the



deployment of Deep Argo floats by US and European partners in the North Atlantic in 2016. The Deep Argo community envisions an array of 1,200 floats at $5^\circ \times 5^\circ$ spacing, capable of sampling the full water column, starting in a few years (Johnson et al. 2015). From its beginning in 1998, Argo's objective has always been to sample the full-depth global ocean. Earlier technology limitations on sampling in marginal seas, seasonal ice-covered oceans, and the deep ocean have all been overcome and a global array is now not only exciting, but also possible.

Figure 3: The four Deep Argo float models: the Deep APEX floats, developed by the University of Washington and Teledyne/Webb; the Deep SOLO floats, developed by Scripps Institution of Oceanography; the Deep NINJA floats, developed by Japan Agency for Marine-Earth Science and Technology (JAMSTEC) and Tsurumi-Seiki Co. (TSK); and the Deep Arvor floats, developed by Institut Français de Recherche pour l'Exploitation de la Mer (IFREMER), Centre National de la Recherche Scientifique (CNRS), and nke Instrumentation.

References

- Aoki, S., S. R. Rintoul, S. Ushio, S. Watanabe, and N. L. Bindoff, 2005: Freshening of the Adélie Land Bottom water near 140 E. *Geophys. Res. Lett.*, **32**, doi:10.1029/2005GL024246.
- Desbruyères, D. G., E. L. McDonagh, B. A. King, F. K. Garry, A. T. Blaker, B. I. Moat, and H. Mercier, 2014: Full-depth temperature trends in the northeastern Atlantic through the early 21st century. *Geophys. Res. Lett.*, **41**, 7971–7979, doi:10.1002/2014GL061844.
- Fahrbach, E., M. Hoppema, G. Rohardt, M. Schroder, and A. Wisotzki, 2004: Decadal-scale variations of water mass properties in the deep Weddell Sea. *Ocean Dynamics*, **54**, 77–91, doi:10.1007/s10236-003-0082-3.
- Fahrbach, E., M. Hoppema, G. Rohardt, O. Boebel, O. Klatt, and A. Wisotzki, 2011: Warming of deep and abyssal water masses along the Greenwich meridian on decadal time scales The Weddell gyre as a heat buffer. *Deep-Sea Res. Part II*, **58**, 2509–2523, doi:10.1016/j.dsr2.2011.06.007.
- Foster, G., and S. Rahmstorf, 2011: Global temperature evolution 1979–2010. *Environ. Res. Lett.*, **6**, 044022–044029, doi:10.1088/1748-9326/6/4/044022.
- Gordon, A. L., 2001: Bottom water formation. *Encyclopedia of Ocean Sciences*, J. Steele, S. Thorpe, and K. Turekian, Eds., Elsevier, 334–340.
- Jacobs, S. S., and C. F. Giulivi, 2010: Large multidecadal salinity trends near the Pacific–Antarctic continental margin. *J. Climate*, **23**, 4508–4524, doi:10.1175/2010JCLI3284.1.
- Johnson, G. C., 2008: Quantifying Antarctic Bottom Water and North Atlantic Deep Water volumes. *J. Geophys. Res.*, **113**, doi:10.1029/2007JC004477.
- Johnson, G. C., J. M. Lyman, and S. G. Purkey, 2015: Informing Deep Argo array design using Argo and full-depth hydrographic section data. *J. of Atmospheric and Oceanic Technology*, submitted.
- Jullion, L., S. C. Jones, A. C. Naveira Garabato, and M. P. Meredith, 2010: Wind-controlled export of Antarctic Bottom Water from the Weddell Sea. *Geophys. Res. Lett.*, **37**, doi:10.1029/2010GL042822.
- Karl, T. R., and Coauthors, 2015: Possible artifacts of data biases in the recent global surface warming hiatus. *Science*, **348**, 1469–1472, doi:10.1126/science.aaa5632.
- Katsumata, K., H. Nakano, and Y. Kumamoto, 2014: Dissolved oxygen change and freshening of Antarctic bottom water along 62°S in the Australian–Antarctic Basin between 1995/96 and 2012/13. *Deep-Sea Res. Part II*, **114**, 27–38, doi:10.1016/j.dsr2.2014.05.016.
- Kosaka, Y., and S.-P. Xie, 2013: Recent global-warming hiatus tied to equatorial Pacific surface cooling. *Nature*, **501**, 403–407, doi:10.1038/nature12534.

- Kouketsu, S., and Coauthors, 2011: Deep ocean heat content changes estimated from observation and reanalysis product and their influence on sea level change. *J. Geophys. Res.*, **116**, doi:10.1029/2010JC006464.
- Kouketsu, S., M. Fukasawa, I. Kaneko, T. Kawano, H. Uchida, T. Doi, M. Aoyama, and K. Murakami, 2009: Changes in water properties and transports along 24°N in the North Pacific between 1985 and 2005. *J. Geophys. Res.*, **114**, doi:10.1029/2008JC004778.
- LeBel, D. A., and Coauthors, 2008: The formation rate of North Atlantic Deep Water and Eighteen Degree Water calculated from CFC-11 inventories observed during WOCE. *Deep Sea Res. Part I: Oceanogr. Res. Papers*, **55**, 891–910, doi:10.1016/j.dsr.2008.03.009.
- Lyman, J. M., and G. C. Johnson, 2014: Estimating global ocean heat content changes in the upper 1800 m since 1950 and the influence of climatology choice*. *J. Climate*, **27**, 1945–1957, doi:10.1175/JCLI-D-12-00752.1.
- Masuda, S., and Coauthors, 2010: Simulated rapid warming of abyssal North Pacific waters. *Science*, **329**, 319–322, doi:10.1126/science.1188703.
- Meehl, G. A., and Coauthors, 2006: Climate change projections for the twenty-first century and climate change commitment in the CCSM3. *J. Climate*, **19**, 2597–2616, doi:10.1175/JCLI3746.1.
- Purkey, S. G., and G. C. Johnson, 2010: Warming of global abyssal and deep Southern Ocean waters between the 1990s and 2000s: Contributions to global heat and sea level rise budgets. *J. Climate*, **23**, 6336–6351, doi:10.1175/2010JCLI3682.1.
- Purkey, S. G., and G. C. Johnson, 2012: Global contraction of Antarctic Bottom Water between the 1980s and 2000s*. *J. Climate*, **25**, 5830–5844, doi:10.1175/JCLI-D-11-00612.1.
- Purkey, S. G., and G. C. Johnson, 2013: Antarctic Bottom Water warming and freshening: Contributions to sea level rise, ocean freshwater budgets, and global heat gain*. *J. Climate*, **26**, 6105–6122, doi:10.1175/JCLI-D-12-00834.1.
- Rhein, M., and Coauthors, 2013: Observations: Ocean. *Climate Change 2013: The Physical Science Basis. Contribution of Working Group I to the Fifth Assessment Report of the Intergovernmental Panel on Climate Change*, Stocker, T. F., D. Qin, G.-K. Plattner, M. Tignor, S. K. Allen, J. Boschung, A. Nauels, Y. Xia, V. Bex and P. M. Midgley, Eds.. Cambridge University Press.
- Swift, J., and A. H. Orsi, 2012: Sixty-four days of hydrography and storms: RVIB Nathaniel B. Palmer's 2011 S04P Cruise. *Oceanogr.*, **25**, 54–55, doi:10.5670/oceanog.2012.74.
- Trenberth, K. E., and J. T. Fasullo, 2010: Tracking Earth's energy. *Science*, **328**, 316–317, doi: 10.1126/science.1187272.
- Trenberth, K. E., J. T. Fasullo, and J. Kiehl, 2009: Earth's global energy budget. *Bull. Amer. Meteor. Soc.*, **90**, 311–323, doi:10.1175/2008BAMS2634.1.

Global warming slowdown—An energy perspective

Ka-Kit Tung¹ and Xianyao Chen²

¹University of Washington

²Ocean University of China

When the global-mean surface temperature did not warm as expected in the presence of ever increasing atmospheric concentration of greenhouse gases that enhance the long-wave radiation to space, there can only be two possible reasons, both involving the energy budget of the earth: (1) the radiative heating was not appreciably reaching the surface - most of it presumably was reflected back to space by, for example, increasing aerosols from volcanoes and anthropogenic pollution; or (2) that the heating was reaching the surface and below, but was sequestered in

the oceans. Of course, a combination of the two is possible. It then follows that no resolution of the “mystery” of the global warming slowdown can be accomplished without a proper accounting of the “missing heat,” including whether any heat was indeed “missing.” The pioneering work of Meehl et al. (2011; 2013) supports hypothesis (2) as a possible explanation. The studies found, at least in the Community Climate System Model version 4 (CCSM4) run under an emission scenario that happens to have an almost constant top of the atmosphere (TOA) radiative imbalance, that the